Chapter 5

RESULTS

5.1 Elastic Wave Velocity of the Chephren amphibolite

Most of the experiments in this study were performed on the Chephren amphibolite, which was investigated parallelly as well as perpendicularly to its foliation. The experiments were done on sample cores which had previously been carefully analysed with respect to their density and open porosity. For these determinations, the cores were saturated with water. Hence, before the ultrasonic experiments the samples were dried for several weeks in a vacuum oven at only 60 °C to minimise microstructural changes due to the heat treatment. Afterwards, samples were stored for several weeks to months at ambient conditions. These samples are referred to hereafter as *air-dry* samples. Two samples were dried again immediately before the experiments and placed directly from the oven into the ultrasonic set-up (*oven-dry* samples). One sample was exposed to an accidental pressure release at 950 MPa (*blow-out*).

5.1.1 Elastic Wave Velocity as a Function of Pressure

Figs. 5.1 a, c, e, and 5.2 a show P wave traveltime traces for several experiments, measured on *air-dry* Chephren amphibolite cores in dependence of pressure. The seismograms are recorded in pulse transmission mode and reflect therefore the sample response to changing experimental conditions. Corrected for the traveltimes in the buffer rods, which decrease linearly with increasing pressure, the P wave velocities of the Chephren amphibolite were determined as described in Chapter 3.1 and are presented in Figs. 5.1 b, d, f and 5.2 b.

In general, traveltimes decrease with increasing pressure, i.e. the velocities increase. Mostly, a non-linearity of velocity with pressure dominates the lower pressure range, which merges into an approximately linear relation above 200 MPa. However, the velocity increase in the non-linear part of the function varies from sample to sample. It is largest for the sample exposed to the *blow-out* (CHE_1), where it increases from 5.27 km/s to 6.09 km/s, corresponding to a relative increase of 15.6 %. (Fig. 5.1 b). For

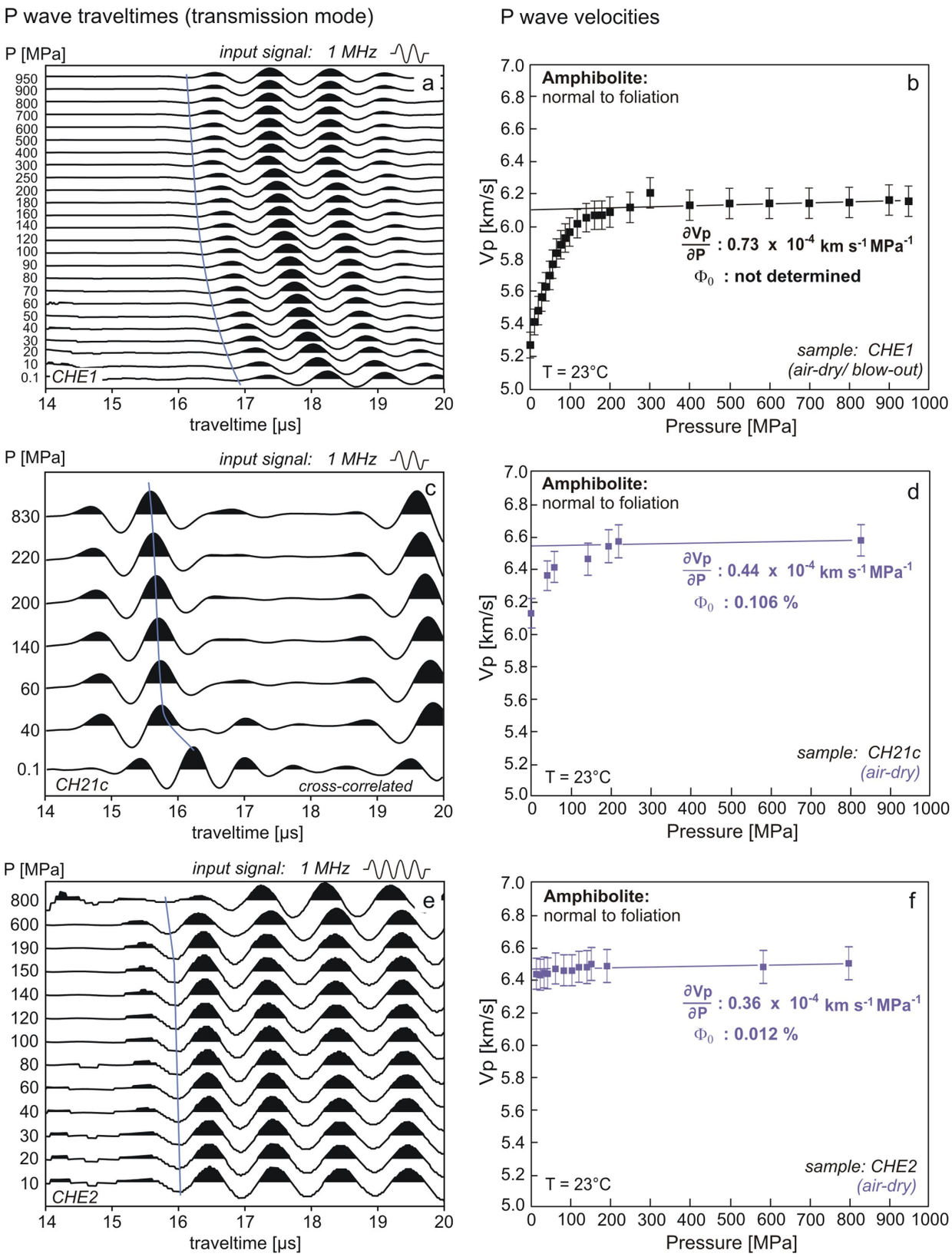

Figure 5.1: *P wave seismograms of Chephren amphibolite, measured perpendicularly to foliation in dependence of pressure (left) and corresponding P wave velocities (right). Seismograms are recorded in pulse transmission mode. Thus P waves run through the whole set-up, consisting of two buffer rods and the sample. Generally, with increasing pressure the traveltimes decline and hence velocities increase. Seismograms (a) and (e) represent unfiltered raw data, while (c) displays cross-correlated traveltime traces. As the signal onset is hard to resolve in this presentation, the first minima of the signal and the maxima of the cross-correlated traces, respectively, are marked by blue lines.* Φ_0 *is the open porosity at ambient PT (see Tab. 4.1).*

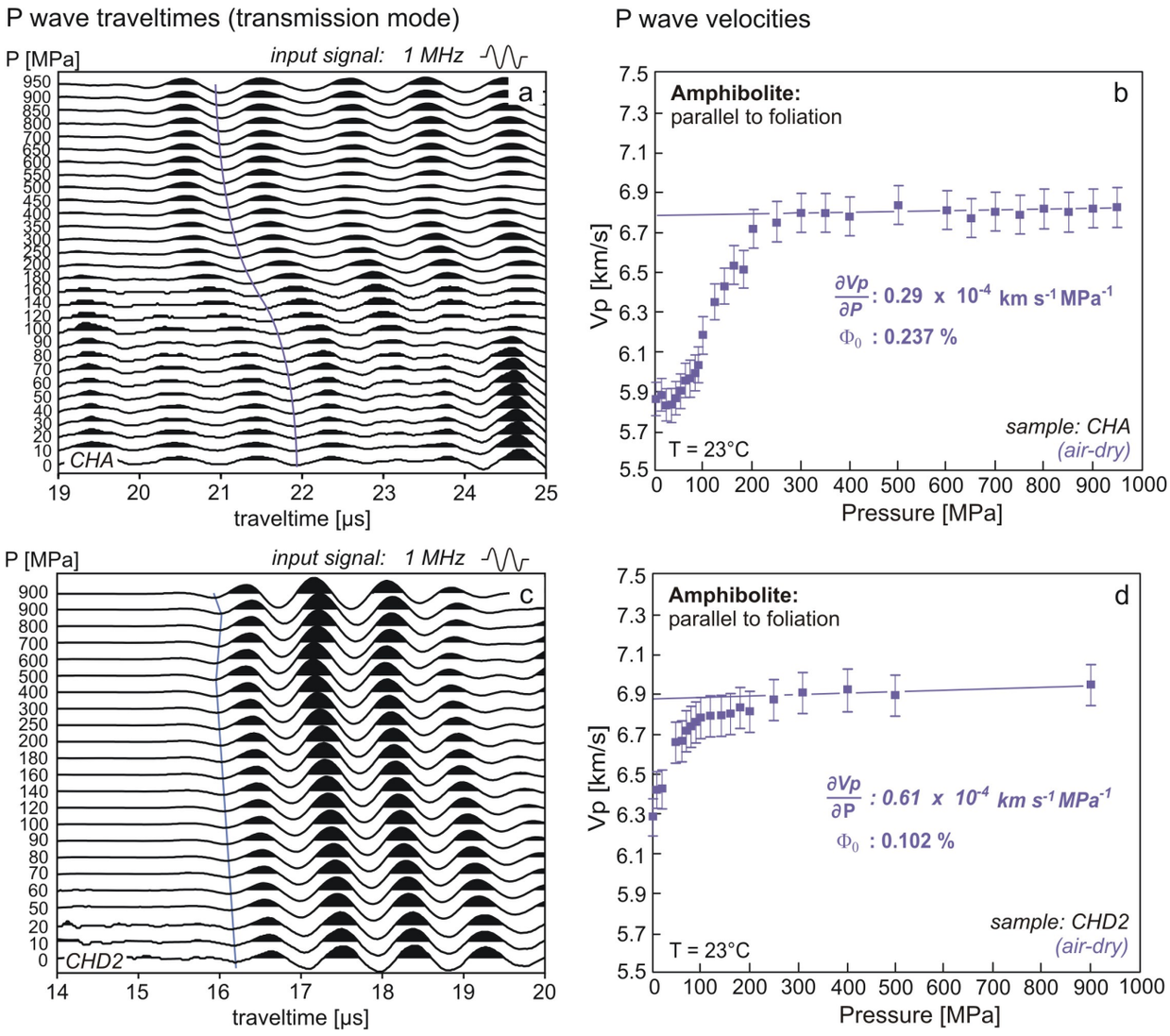

Figure 5.2: *P wave seismograms of Chephren amphibolite measured parallel to the foliation and lineation (left) and the corresponding P wave velocity as a function of pressure (right). Here buffer rods of ZrO_2 were used, which results generally in larger traveltimes of the transmitted wave.* Φ_0 *is the open porosity at ambient PT.*

sample CH_A an open porosity of 0.24 % was determined (Tab. 4.1). In this case the change in velocity is also large, as v_p increases from 5.82 km/s to 6.72 km/s or about 14.8 %. In contrast, it tends to almost zero for sample CHE_2, with only 0.012 % open porosity (Fig. 5.1 f). In the latter case, only slight variations from the linear trend are observed at pressures $<$ 200 MPa. Here, the relative increase of velocity is less than 1 % from 6.45 km/s to 6.50 km/s.

For all datasets characterised by an increasing v_p–pressure relation a least squares fit line was calculated for the linear part of the functions between 200 MPa and the highest pressure value ($(\partial v_p/\partial P)_T$; Fig. 5.1). For the datasets measured perpendicularly to the foliation the pressure derivatives vary between 0.33 $\times 10^{-4}$ and 0.46 $\times 10^{-4}$ $[km\ s^{-1}MPa^{-1}]$. From regression lines the intrinsic velocity ($v_{p_{min}}$) at room temperature and 1 bar pressure (*ambient conditions*) is in the range of 6.47 to 6.53 km/s. Sam-

ple CHE_1 (*blow-out sample*) is an exception, as it shows generally significantly lower velocities than the other samples measured normal to the foliation. Furthermore, here a steeper $(\partial v_p/\partial P)_T$ of 0.73 $\times 10^{-4}$ $[km\ s^{-1} MPa^{-1}]$ is observed.

From measurements parallel to the foliation (Fig. 5.2 b, d) a mean intrinsic velocity of 6.84 km/s ($v_{p_{max}}$) was derived for *ambient conditions*, representing the maximum velocity due to the texture (LPO) of the sample. The pressure derivatives derived from experimental data vary between $(\partial v_p/\partial P)_T$ = 0.29 $\times 10^{-4}$ and 0.61 $\times 10^{-4}$ $[km\ s^{-1} MPa^{-1}]$.

The anisotropy A of P wave velocities was determined with 4.68 %, obtained from $v_{p_{max}}$ and $v_{p_{min}}$ at ambient conditions:

$$A\,[\%] = \frac{v_{p_{max}} - v_{p_{min}}}{v_{p_{max}}} \cdot 100. \tag{5.1}$$

As with increasing pressure the S waves slide into sidewall reflections (see Chapter 3.2), the accurate picking of their onset-times is problematic. For this reason, S wave data are considered only when possible (Fig. 5.3 b). Under the assumption that the onset of the S waves was determined correctly, the increase of v_s up to 300 MPa is slightly restrained compared to the v_p data. This results in an apparently discontinuous development of v_p/v_s. Between 0.1 and 40 MPa v_p/v_s increases steeply from 1.64 to 1.69 and changes into a declining trend between 40 and 300 MPa. At 600 and 850 MPa the decrease of v_p/v_s intensifies. However, here the decrease of P and S wave velocities is the crucial factor.

A decrease of elastic wave velocities was observed in some experiments at pressures > 500 *MPa* (e.g. Fig. 5.3). The corresponding increase in traveltimes occur only in pulse transmission data and not in pulse echo recordings. Hence, it is concluded that changes in the sample account for this surprising behaviour, which might be traced back to experimental constraints. As described in Chapter 3.1 the equilibration time for the system, at which the pressure was held constant, was 45 min. If this time span was significantly enlarged from 45 min to several days an increase in velocity was noticed (Fig. 5.3 f). On sample *CHD2* the measurement at 900 MPa was repeated after 56 h, whereby a relative increase of velocity by about 5 % arises (Fig. 5.3 f). In other cases with a shorter waiting time (12 to 24 h) a minor increase was observed. For experiments, which were performed after the above mentioned *blow-out* long-lasting equilibrations of the system for several days were impossible for safety reason (Fig. 5.3 a and b).

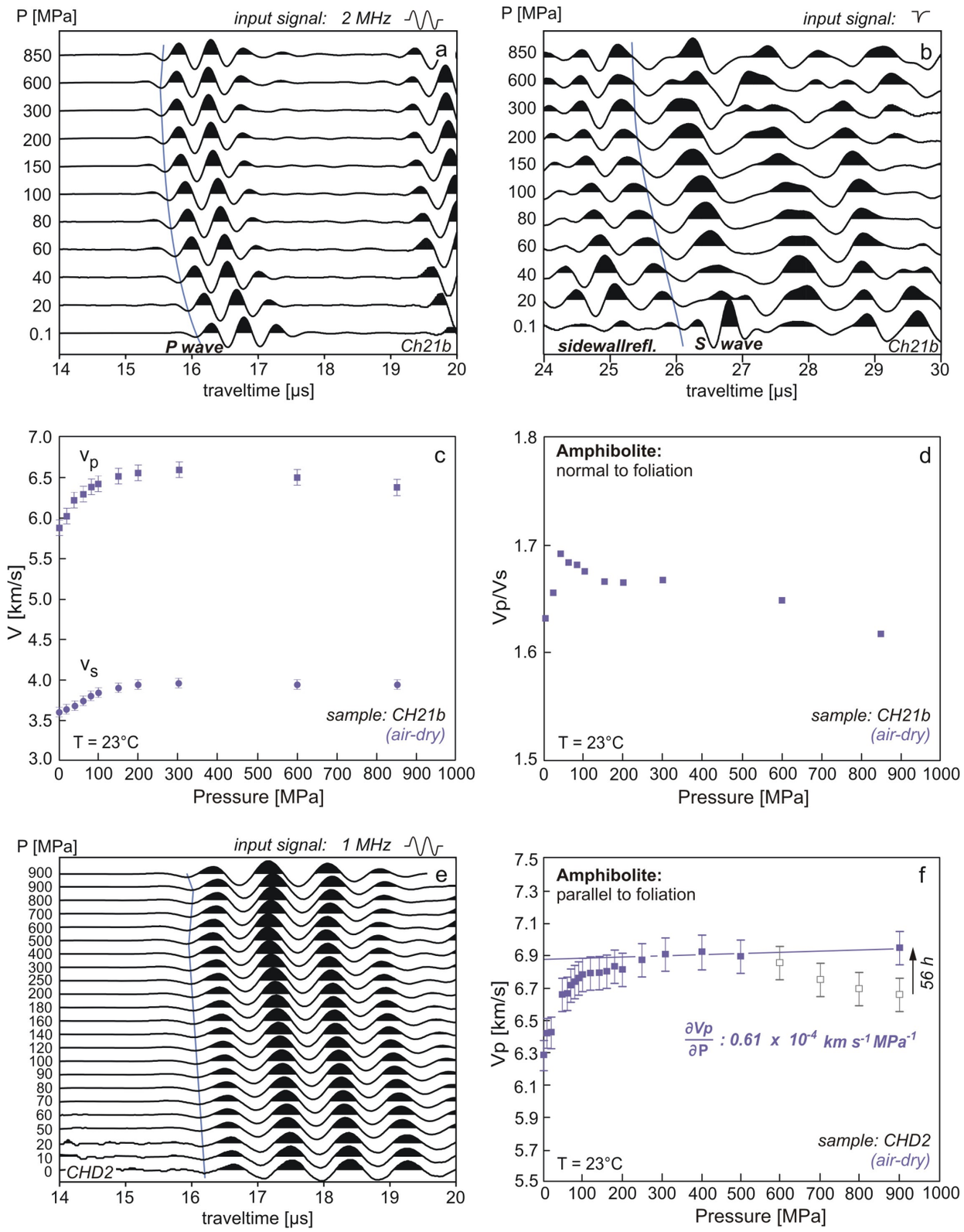

Figure 5.3: *(a) and (b) represent time windows of P and S phases of Chephren amphibolite (normal to the foliation) as functions of the pressure. With increasing pressure the S wave interferes with sidewall reflections and is thus considered only in exceptions. (c) and (d) display the derived elastic wave velocities (left) and the v_p/v_s ratio, respectively. No $(\partial v_p/\partial P)_T$ were derived from these data, because velocities decrease at higher pressures. (e) and (f) show P wave traveltime traces as function of increasing pressure and the corresponding P wave velocities. All measurements were started after 45 min of constant pressure conditions. After 56 h the measurement at 900 MPa was repeated. Note the increase of the velocity with waiting time. Seismograms represent unfiltered raw data. The blue lines in the seismograms mark the first minima of the P wave signals and the signal onset of the S waves.*

5.1.2 Elastic Wave Velocity as a Function of Temperature

When matter is heated, it usually expands. To suppress the development of thermally induced microcracks due to different thermal expansion coefficients of the rock-forming minerals, all temperature experiments were conducted under a high confining pressure between 750 and 900 MPa. Different experiments were performed to investigate variations of the elastic behaviour of Chephren amphibolite as a function of temperature with various sample arrangements:

(I) Several runs were carried out on fluid-tight encapsulated *air-dry cores*, which were measured parallelly and perpendicularly to the foliation (Figs. 5.4 and 5.5 a and b). For both orientations the general characteristics of the velocity–temperature relation are quite similar. Already in the low-temperature range ($<$ 450 °C) a substantial relative decrease of velocity by 6.5 – 9 % was observed. For measurements *normally* to the foliation plane, the temperature derivatives $(\partial \mathrm{v}_p/\partial T)_P$ vary significantly between -1.09×10^{-3} $[km\ s^{-1}\ °C^{-1}]$ and -1.64×10^{-3} $[km\ s^{-1}\ °C^{-1}]$. It was found, that the sample with the strongest increase of velocity at pressures below 200 MPa (sample CHE_1) is characterised by a considerably flatter $(\partial \mathrm{v}_p/\partial T)_P$ than sample CHE_2, which is dominated by an approximately linear velocity–pressure relation (compare with Fig. 5.1). At higher temperatures the strong decrease of velocities is stopped. In most cases velocities re-increase in a distinct temperature interval of about 150 K and then decline again. For the individual experiments the onset of the velocity re-increase varies between 300 and 450 °C and seems to be related to $(\partial \mathrm{v}_p/\partial T)_P$ of the low temperature range: The more negative the value of $(\partial \mathrm{v}_p/\partial T)_P$, the lower is the temperature of the velocity re-increase. – The velocity measurement *parallel* to the foliation gave corresponding results, and a temperature derivative of -1.23×10^{-3} $[km\ s^{-1}\ °C^{-1}]$ was determined.

(II) To investigate the influence of fluid drainage on the seismic signature of the Chephren amphibolite, an additional experiment on an air-dry sample was run with fluid traps integrated into the encapsulated sample assembly (Fig. 5.5 c and d). The fluid traps consisted of cavities, milled into the buffer rods, which were filled with diamond powder (500 μm) to ensure a certain porosity even under high confining pressure. However, the utilisation of the fluid traps did not vary the trend of the velocity–temperature relation and a similar $(\partial \mathrm{v}_p/\partial T)_P$ of -1.30×10^{-3} $[km\ s^{-1}\ °C^{-1}]$ is observed as for samples without fluid trap. At temperatures between 400 and 700 °C, v_p changes in a ”zigzag” trend, as the first re-increase/ re-decrease is followed by a second velocity re-increase above 650 °C.

(III) The experiments were repeated with samples heated in the oven for 24 h at 60 and 120 °C, respectively, to significantly reduce the amount of residual water in the pore space. (Fig. 5.5 e and f). In both cases the general trend is identical to those of non-tempered samples, but the reduction of velocity is less pronounced. In addition $(\partial \mathrm{v}_p/\partial T)_P$ seems to be dependent on the temperature at which the samples were dried. For the sample tempered at 60 °C, a $(\partial \mathrm{v}_p/\partial T)_P$ of -1.07×10^{-3} $[km\ s^{-1}\ °C^{-1}]$ was de-

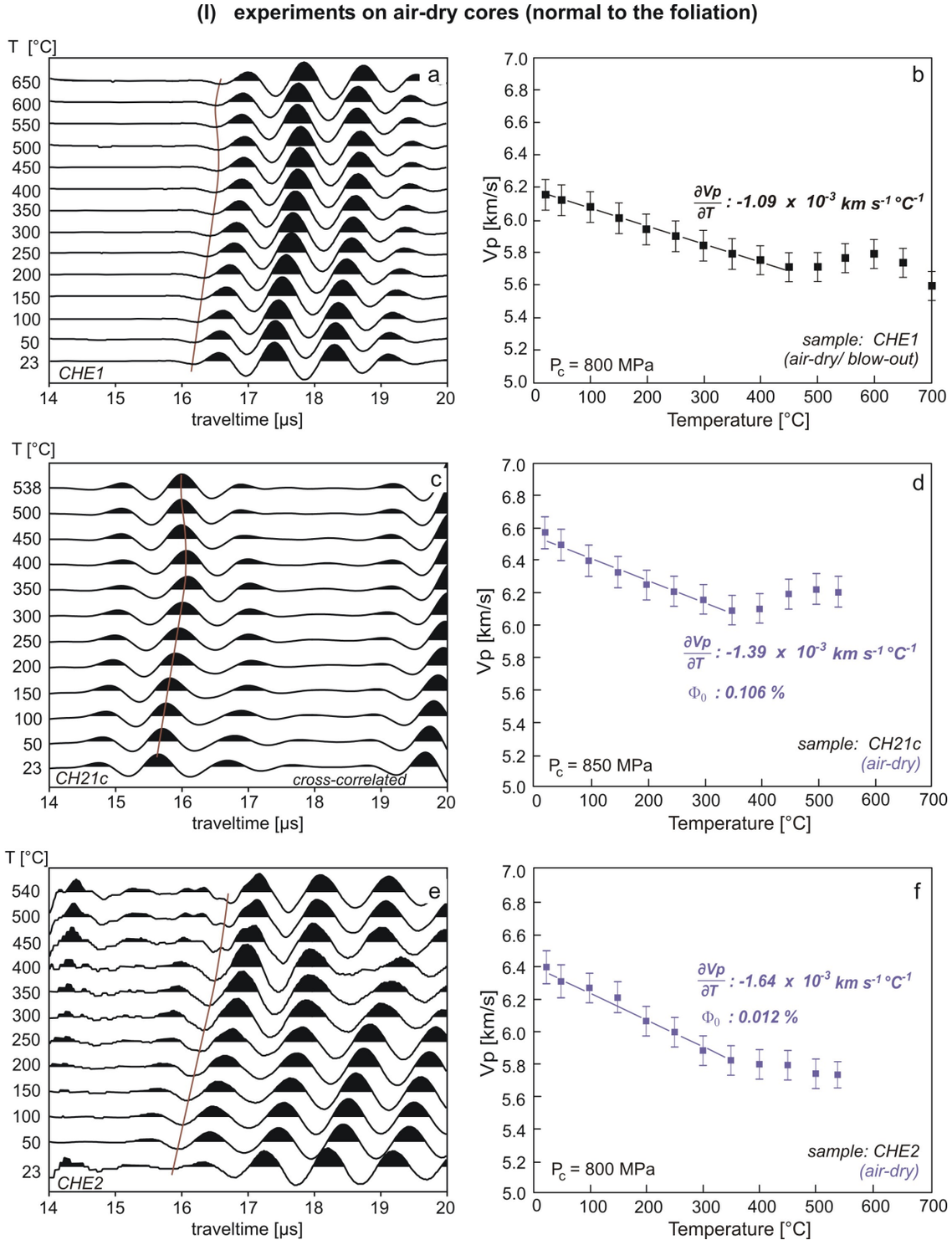

Figure 5.4: *P wave seismograms of Chephren amphibolite, measured perpendicularly to foliation as function of temperature (left) and corresponding P wave velocities (right). Seismograms are recorded in pulse transmission mode. Red lines in the seismogram plots mark the first minima of the signal and the maxima of the cross-correlated traces, respectively. Generally, with increasing temperature an increase of the traveltimes can be observed, thus velocities decrease. However, at higher temperatures this trend is inverted and the velocities increase. Between 450 – 600 °C a re-decrease of traveltimes appears.*

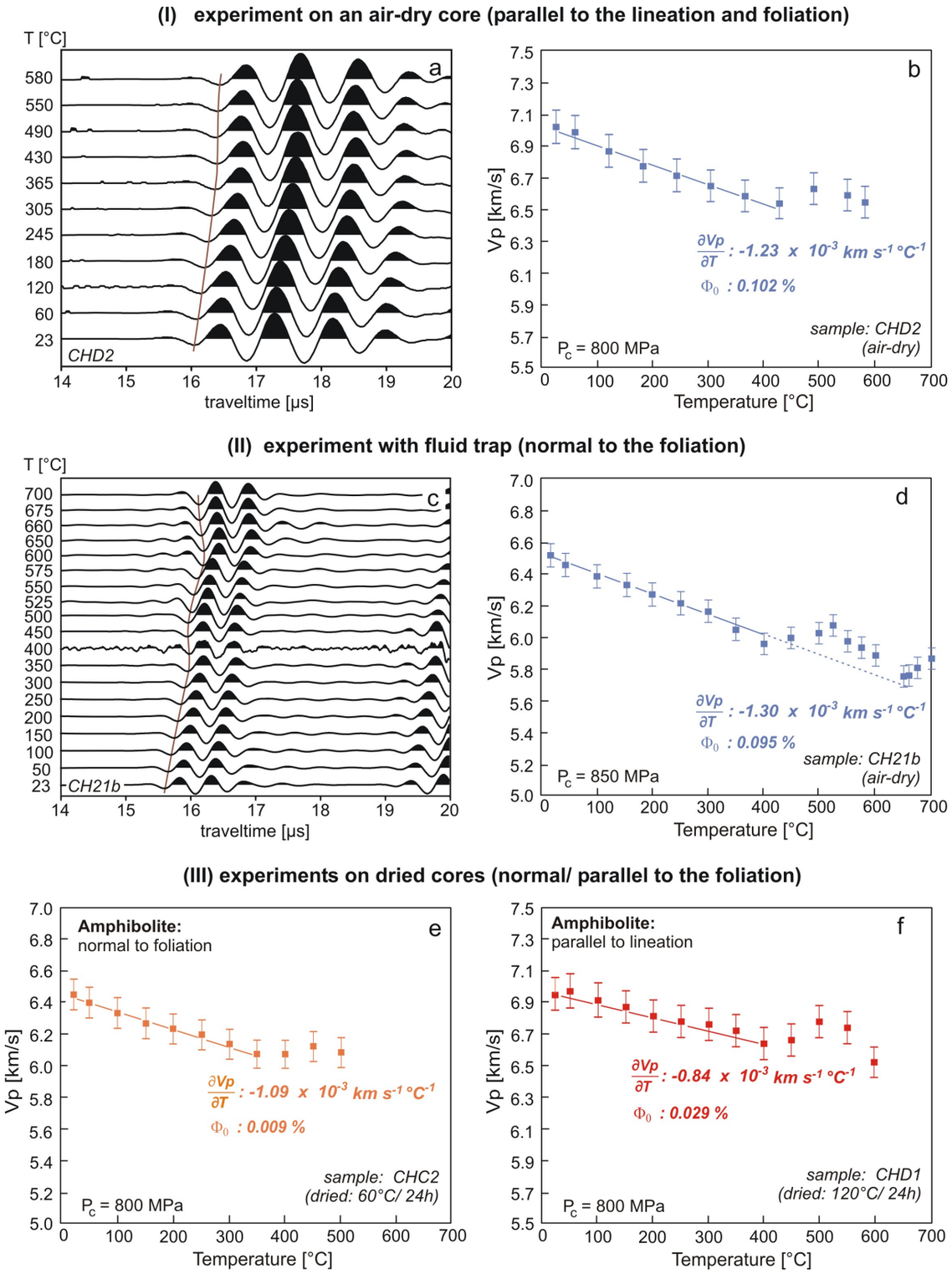

Figure 5.5: *P wave seismograms (a; c) and corresponding P wave velocities (b; d) of Chephren amphibolite as function of temperature. Seismograms are recorded parallelly to the lineation in pulse transmission mode. The red line in the seismogram plot mark the first minima of the signal. Generally, with increasing temperature an increase of the traveltimes can be observed, thus velocities decrease. However, at higher temperatures this trend is inverted and the velocities increase. Between 450 – 600 °C a re-decrease of traveltimes appears. (e; f) Experiments on oven-dry samples. Note that the higher the drying temperature was, the more moderate is the decrease of velocity.*

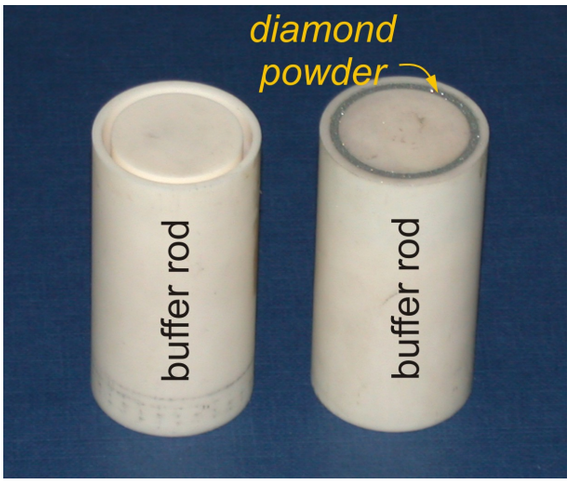

Figure 5.6: *The fluid traps consist of circumferential cavities milled 15 mm deep into the buffer rods. To stabilise the trap and ensure a high porosity at high confining pressure it is filled with diamond powder. After the filling, the buffer rods are dried at 60 °C for 24 h to avoid the introduction of moisture into the system by the large surface of fluid traps.*

termined, while for the sample dried at 120 °C a temperature derivative of -0.83×10^{-3} $[km\ s^{-1}\ °C^{-1}]$) was observed. However the re-increase of velocity as well as the second velocity decrease occur at the same temperatures as observed for the non-tempered samples.

In summary, three to four stages can be discerned in the temperature dependence of P wave velocities: (1) a linear decrease of the velocity, wereby the slope seems to depend on the degree of dryness of the samples and the initial porosity, (2) a re-increase of velocity, and (3) a second decrease of velocity, which is usually steeper than in *stage 1*. In one experiment heated to higher temperatures (700 °C), additionally a second re-increase was observed (4).

No correlation was found between the steepness of the slope and the applied confining pressure, which varies between 750 to 900 MPa for several experiments. Also, there seems to be no distinct dependence between the slope and the sample orientation with regard to its textural anisotropy (foliation). Furthermore, there is no constant critical temperature for the reversion of the v_p–temperature trend, but both, the slope and the onset of velocity re-increase seem to be a function of the initial porosity of the sample: The higher the initial porosity of the rock sample is, the less pronounced is the velocity reduction in *stage 1* and the later the onset of *stage 2* is observed. However, the greatest effect on the degree of velocity reduction apparently is the tempering of the samples. Experiments with dried samples (T = 60 and 120 °C) corroborate an admittedly reduced decrease of velocity with increasing drying temperatures.

The Influence of Time-Variant Data Recording

The amphibolite was investigated additionally in terms of time-variant changes of its elastic behaviour. For this reason, at each temperature step the measurements were repeated in intervals of 10 min. Fig. 5.7a displays the recorded signals over a time span of 30 min. The incident signal for the *20-minute trace* was a needle impulse, while for the *10-* and *30-minute traces* a 2 MHz – two-wavelet sinus signal was transmitted through the set-up. In this case the signals can be compared directly.

Up to 350 °C (*stage 1*), the declining velocity–temperature relations for all three time-intervals are almost congruent and $(\partial v_p/\partial T)_P$ is nearly constant (-1.26×10^{-3} $[km\ s^{-1}\ °C^{-1}]$ after 10 minutes, -1.20×10^{-3} $[km\ s^{-1}\ °C^{-1}]$ after 30 min). However, at temperatures $\geq$ 400 °C slight variations could be resolved. When reaching the transition from *stage 1* to *stage 2* with the re-increase of velocity, slightly higher velocities are observed with increasing duration. The maximum variation between first and last determined velocity is 0.55 % at 450 °C and 0.95 % at 500 °C.

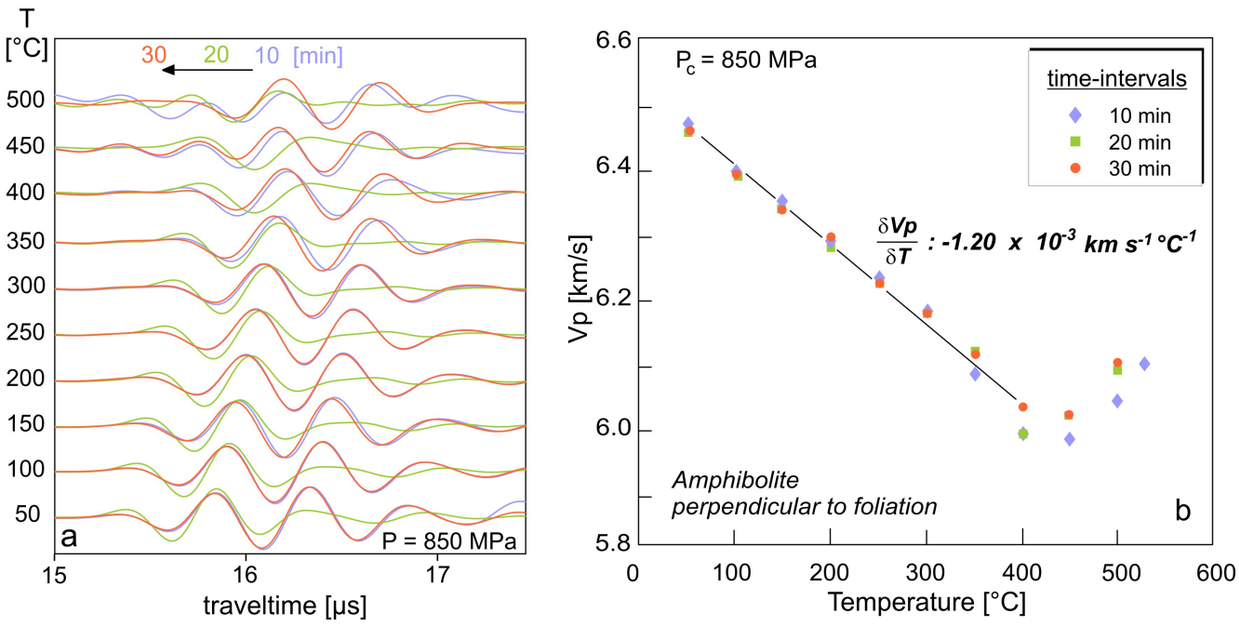

Figure 5.7: *(a) P wave traveltimes (zero-phase filtered transmission signals) of the Chephren amphibolite recorded as a function of time delayed after reaching the respective temperatures. The 10 and 30 minutes-records (blue and red traces) refer to a 2 MHz–two wavelet sinus, the 20 minutes records (red) to a needle impulse. Note the concordance of the blue and red traces up to 250 °C and the shift at higher temperatures. (b) Comparison of calculated velocities for all three time intervals. The experiment was performed with fluid traps integrated into the buffer rods.*

5.2 Elastic Wave Velocity of the Malenco Serpentinite

5.2.1 Elastic Wave Velocity as a Function of Pressure

One experiment was conducted on serpentinite. The initial porosity of the sample was determined to be 0.178 %. Compressional as well as shear waves were recorded parallel to foliation of an *air-dry* sample (Fig. 5.8). In anisotropic media shear waves split up into two waves of different velocities oscillating orthogonally to each other. Due to the limited number of electric lead-throughs here only the faster S wave was recorded.

For serpentinite only few pressure steps could be realised due to leakage problems of the pressure vessel. In particular, between 250 and 840 MPa no further pressure steps were realised. Nonetheless,

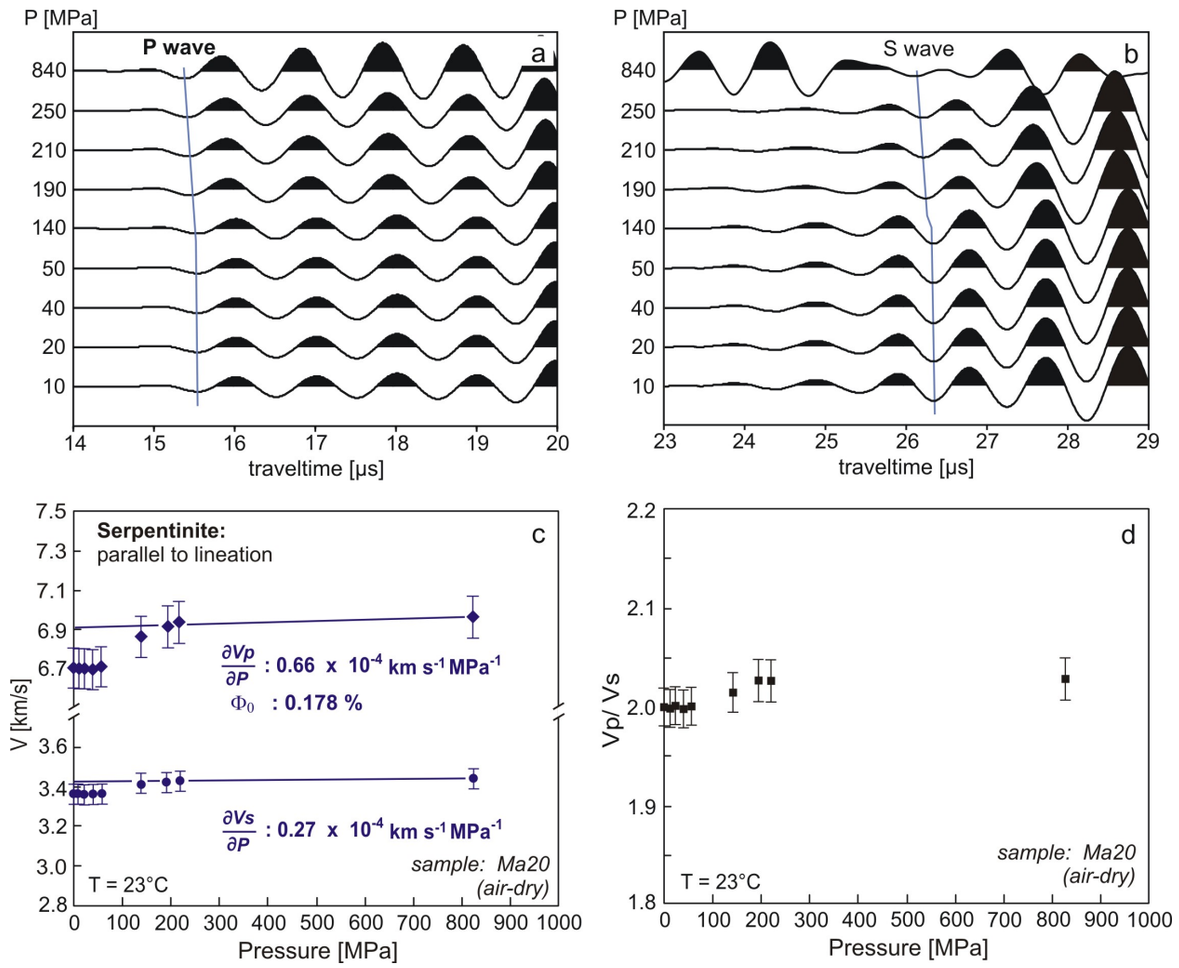

Figure 5.8: *(a and b) Zero-phase filtered P and S wave traveltime traces of Malenco serpentinite in dependence of pressure. (c) P and S wave velocities of Malenco serpentinite as a function of pressure. The error is assumed to be ± 1.5 % (2 σ). (d) v_p/v_s as a function of pressure. The error is ± 1 % (2 σ). Φ_0 is the open porosity at ambient PT.*

traveltimes of compressional and shear waves clearly reduce with increasing pressure. In consequence, the P wave velocity increases in the first 200 MPa from 6.72 km/s to 6.93 km/s, which is a relative increase of 3.0 %. In the same pressure range the shear wave velocity increase from 3.36 km/s to 3.42 km/s, which corresponds to a relative velocity increase of about 1.6 %. This results in an increasing v_p/v_s ratio (Fig. 5.8 d). The best-fit solutions of the serpentinite data between 190 to 830 MPa are $v_p = 7.10\ km/s$ and $v_s = 3.42\ km/s$. The pressure derivatives determined between 190 and 840 MPa are $(\partial v_p/\partial P)_T = 0.66 \times 10^{-4}\ [km\ s^{-1} MPa^{-1}]$ and $(\partial v_s/\partial P)_T = 0.27 \times 10^{-4}\ [km\ s^{-1} MPa^{-1}]$, respectively. The derivatives give a v_p of 6.93 km/s and a v_s of 3.42 km/s at ambient conditions.

5.2.2 Elastic Wave Velocity as a Function of Temperature

In contrast to the measurements on the Chephren amphibolite, the velocity–temperature relation of the Malenco serpentinite is characterised by only a slight decrease of P and S wave velocities, which is nearly linear up to 600 °C for both wave types (Fig. 5.10). The temperature derivatives were determined with $-0.60 \times 10^{-3}\ [km\ s^{-1}\ °C^{-1}]$ for P waves and $-0.46 \times 10^{-3}\ [km\ s^{-1}\ °C^{-1}]$ for S waves, both extracted from least square fits between 23 and 600 °C. However, at temperatures higher than 650 °C the P wave velocity dramatically decreases within a temperature interval of 50 K from 6.49 km/s to 5.86 km/s, which corresponds to a relative velocity decrease of about 10 % (Fig 5.10 c). The reduction of the shear wave velocity is less pronounced in the same temperature range, changing from 3.30 km/s to 3.11 km/s, which corresponds to 6 % (Fig 5.10 c). Despite the predominantly small variations of compressional and shear

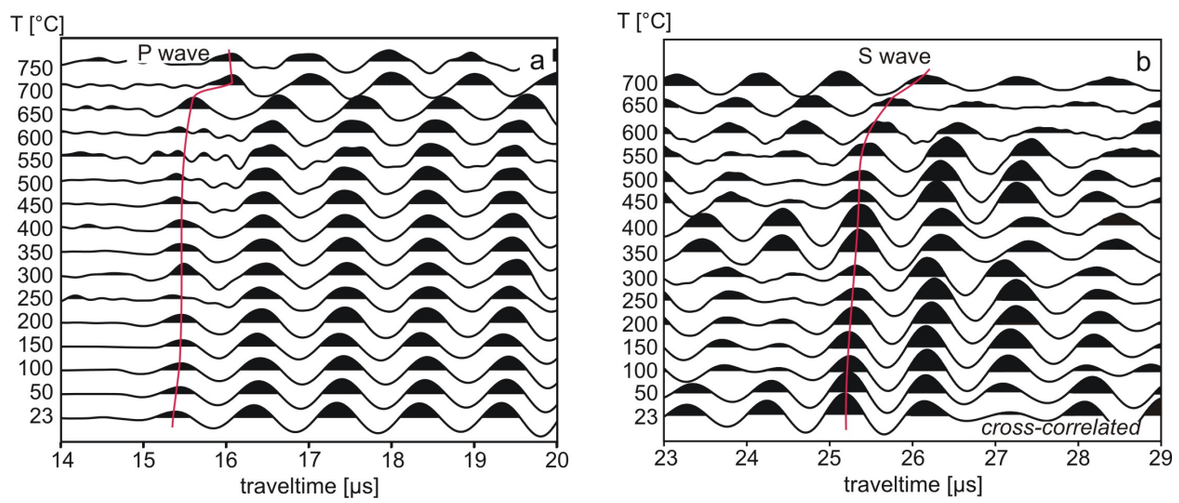

Figure 5.9: *Traveltime traces of the Malenco serpentinite as a function of temperature.(a) P wave traces are low-pass filtered. (b) Due to noisy signals the S wave data are cross-correlated.*

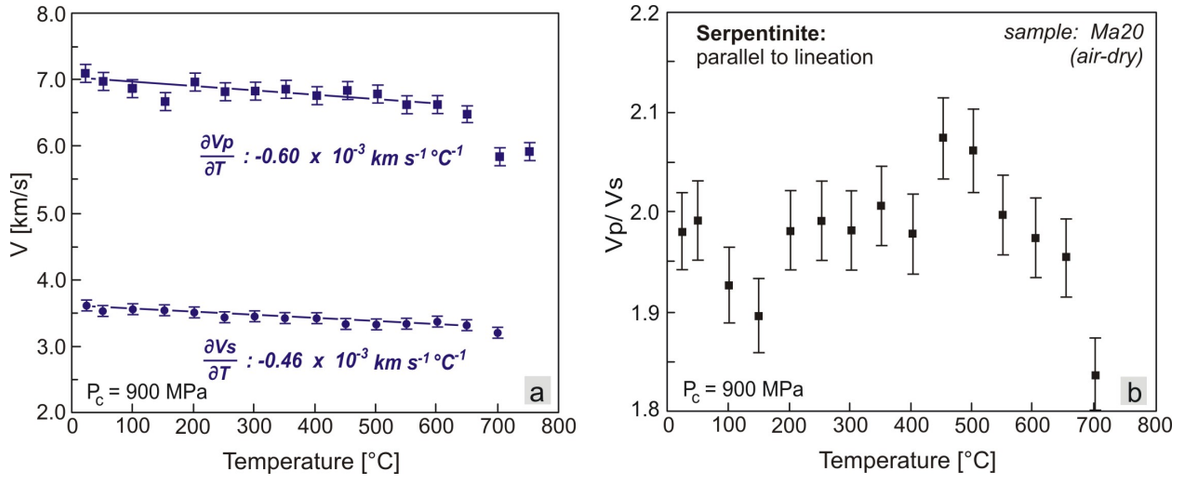

Figure 5.10: *(a) P and S wave velocities as a function of temperature. Due to noisy signals during the temperature run the data were applied to an enhanced processing procedure. This results in an error of ± 2 % compared to an error of ± 1.5 % for the amphibolite velocities. (b) v_p/v_s ratio (2σ = ± 2 %) as a function of temperature.*

wave velocities the v_p/v_s ratio (Fig 5.10 d) points to a strong temperature dependence. Between 50 and 150 °C v_p/v_s decreases by about 4 % and returns to a medium value of 1.98 at 200 °C. At 450 °C v_p/v_s increases rapidly by about 4 % to decrease finally significantly again.